Molecular Crystals and Liquid Crystals
Publication details, including instructions for authors and subscription information:
http://www.tandfonline.com/loi/gmcl20

Effect of Surface Treatment on the Efficiency of Bulk Hetero-Junction Solar Cells Prepared on Low-Temperature Processed Titanium Dioxide Fim

Eiji Itoh [a] , Yuta Takamizawa [a] & Keiichi Miyairi [a]
[a] Department of Electrical and Electronic Engineering, Faculty of Engineering, Shinshu University, Wakasato, Nagano, Japan

Version of record first published: 25 Jun 2009

To cite this article: Eiji Itoh, Yuta Takamizawa & Keiichi Miyairi (2009): Effect of Surface Treatment on the Efficiency of Bulk Hetero-Junction Solar Cells Prepared on Low-Temperature Processed Titanium Dioxide Fim, Molecular Crystals and Liquid Crystals, 504:1, 104-113

To link to this article: http://dx.doi.org/10.1080/15421400902939587

Mol. Cryst. Liq. Cryst., Vol. 504, pp. 104–113, 2009
Copyright © Taylor & Francis Group, LLC
ISSN: 1542-1406 print/1563-5287 online
DOI: 10.1080/15421400902939587

Effect of Surface Treatment on the Efficiency of Bulk Hetero-Junction Solar Cells Prepared on Low-Temperature Processed Titanium Dioxide Fim

Eiji Itoh, Yuta Takamizawa, and Keiichi Miyairi
Department of Electrical and Electronic Engineering, Faculty of Engineering, Shinshu University, Wakasato, Nagano, Japan

We have fabricated the bulk hetero-junction organic solar cells consisting of PCBM and P3HT blend on flat, and dense, low-temperature (<150°C) processed anatase titanium oxide film obtained by sol-gel process. The photovoltaic properties were markedly improved by the insertion of MoO_3 layer between active layer and Au (or Ag). The photovoltaic properties of solar cell on non-treated low-temperature titanium oxide, however, markedly decreases compared with the cell on high-temperature processed titanium dioxide probably due to the dense surface defects on the low-temperature titanium oxide. Therefore, we have treated the surface of titanium oxide by fullerene based self-assembled monolayer (C_{60}-SAM) using aminopropyl-ethoxysilane and C_{60}. The photovoltaic properties of polymer BHJ cells on surface treated low-temperature titanium oxide was improved markedly probably due to the passivation of surface defects on low-temperature processed titanium oxide films, such as -OH etc. and improved electron transfer between titanium oxide and active layer.

Keywords: bulk-hetero junction; fullerene SAM; low-temperature process; MoO_3; solar cell

1. INTRODUCTION

Printable, flexible and low-cost organic semiconductors are of great interest for potential low-cost solar cells. Particularly, bulk-heterojunction (BHJ) polymer solar cells is a promising candidate

---

This work was supported by the CLUSTER of the Ministry of Education, Culture, Sports, Science and Technology, Japan, and Research Foundation for the Electrotechnology of Chubu (R-18229).

Address correspondence to Eiji Itoh, Department of Electrical and Electronic Engineering, Shinshu University, 4-17-1 Wakasato, Nagano, Japan. E-mail: eitoh@shinshu-u.ac.jp

because of low-cost fabrication in large area by a solution process or printing techniques on plastic substrates, and the power conversion efficiencies have reached 3–5% in a single cell structure, recently [1–9]. On the other hand, crystalline TiO_2 is well known as a wide-gap semiconductor, which is transparent for visible light, and as an n-type semiconductor with a large electron affinity, which is suitable for photocatalysis [10], and for solar energy converters [11–16]. However, crystallization of TiO_2 usually requires a high-temperature heat treatment above 450°C by sol-gel techniques. Recently, Kim *et al.* and Hayakawa *et al.* prepared a polymer BHJ cell with an efficiency of 4–5% by an insertion of very thin amorphous TiOx layer, and they showed the higher air-stability and longer-lifetime [8,9]. Although, the use of very thin amorphous TiOx layers instead of thicker crystalline TiO_2 films seems to be a useful method, the establishment of a fabrication process for crystalline TiO_2 films at a temperature lower than 150°C by the sol-gel route [17–19] or sputtering techniques [20] is the recent trend in the field of organic solar cell application as well as photocatalysis.

In this study we prepared crystalline TiO_2 (anatase phase) thin film by a high-temperature process and a low-temperature process at a temperature not higher than 150°C by sol-gel techniques. We then fabricated BHJ cell on these TiO_2 films consisting of regioregular poly (3-hexylthiophene) (P3HT) and [6,6]-phenyl C61 butyric acid methyl ester (PCBM) as a active layer. We also investigated the effect of the MoO_3 hole buffer layer and the self-assembled monolayer (SAM) of fullerene, which is deposited on low-temperature processed TiO_2 in order to reduce the electron traps, on the photovoltaic properties of BHJ solar cells.

2. EXPERIMENTAL

Titanium-tetraisopropoxide (TTI) was used as a starting material, and nitric acid (Wako Pure Chemical Industries) as a peptizer. The refluxed sol of TTI with water and nitric acid was prepared by the process reported Yun *et al.* [17]. That is a mixture of TTI (6 ml, 0.024 mol) and ethanol (1 ml) was added to de-ionized water (40 ml) and then nitric acid (0.4 ml) was added to the TTI solution. The resulting sol was refluxed at 80°C for 8 h with vigorous stirring, producing a milky solution. This sol (10 ml) was then diluted with ethanol (20 ml) for the better wettability and reduction of damage to the under-layer [19]. TiO_2 thin films were then transferred onto ITO-coated glass substrates by the dip-coating technique at a drawing speed of 100 mm/min. Here the width of Indium Tin Oxide (ITO) was 2 mm and the sheet resistance of ITO was 15 Ω/sq. TiO_2 films were then heat-treated at 150°C or 500°C for 1 h in atmosphere. We defined the low-temperature processed TiO_2 film at 150°C as L-TiO_2 and the high-temperature processed TiO_2 film at 500°C as H-TiO_2, respectively. All samples were then paddled in de-ionized water and ethanol for 2 minutes. The surface of L-TiO_2 films were also treated by self-assembled monolayer (SAM) of 3-aminopropyl-triethoxysilane (APTES) in toluene, and then treated again by fullerene C_{60} in toluene at 80°C if it is necessary [21]. The crystalline phase of TiO_2 was identified from X-ray diffraction patterns. We chose a mixture of P3HT and PCBM (1:0.8 in wt%) as the active layer and it was spin-coated from 2 wt% of chlorobenzene solution, and then the 2-mm-wide MoO_3 buffer layer, and Au or Ag top electrode was evaporated. Here, the effective electrode area was 4 mm^2. The thickness of L-TiO_2, H-TiO_2, active layers, MoO_3, Au, and Ag films were 100 ~ 200 nm, 50 nm, 100 nm, 30 nm, 30 nm and 30 nm, respectively.

The current-voltage (*I*-*V*) characteristics under illumination were then measured in a vacuum chamber at 30°C using a source meter (Keithley 2400) and a 100 W Xenon arc lamp with an optical filter to obtain the AM-1.5-like spectrum. The intensity of the incident light to the sample was 70 mW/cm^2. Here, the sample was illuminated through the transparent ITO side, and the sample was also measured after heat-treatment at various temperatures of 50, 75, 100, 125, and 150°C for 30 min. The forward bias was applied to the top electrode with respect to ITO.

3. RESULTS AND DISCUSSION

Figure 1 shows the X-ray diffraction patterns of titanium oxide films heat-treated at 150°C (L-TiO_2), and 500°C (H-TiO_2) for 1 h. It is noted here that the sol-gel processed TiO_2 film heat-treated at a low temperature usually becomes amorphous, and the anatase crystalline form appears only after sintering the film at a high temperature of about 500°C. However, both films sintered at 150°C and 500°C show the strong (101) peak and (200) peak corresponds to anatase TiO_2 [11–16]. That is, this process seems to be compatible with flexible device applications and the preparation of TiO_2 layers on polymer-based semiconductors.

Figure 2 shows the I-V curves of ITO/H-TiO_2/P3HT + PCBM/Au device as a parameter of the heat-treatment temperature under illumination. It is clearly shown that the photovoltaic properties were improved markedly by heat-treatment up to 75°C probably due to the crystallization of P3HT in the active layer as shown in Figure 3. On the other hand, the photovoltaic properties deteriorate gradually

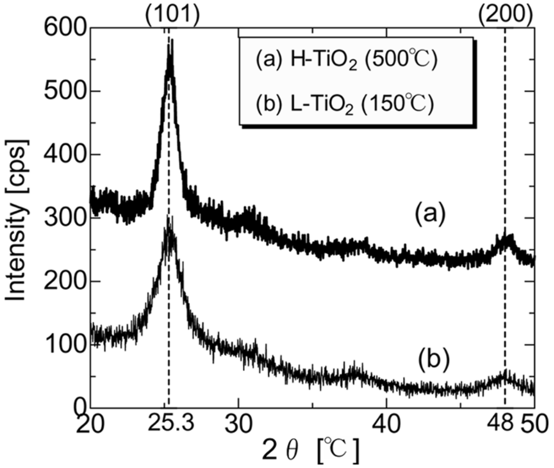

FIGURE 1 The X-ray diffraction patterns of titanium oxide films heat-treated at 150°C (L-TiO_2), and 500°C (H-TiO_2) for 1 h.

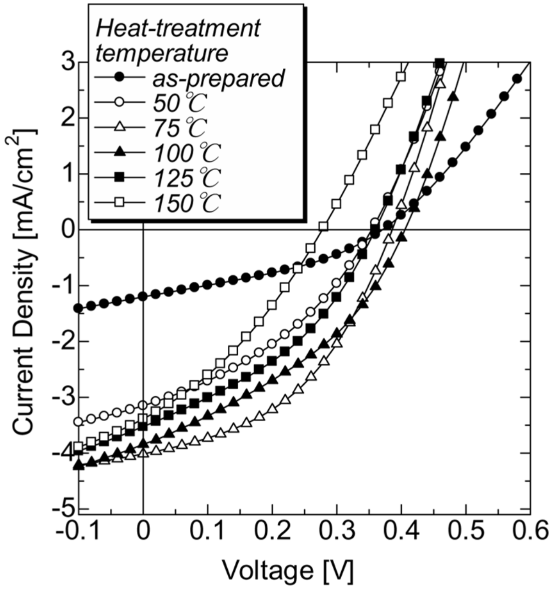

FIGURE 2 The I-V curves of ITO/H-TiO_2/P3HT + PCBM/Au device as a parameter of the heat-treatment temperature under illumination.

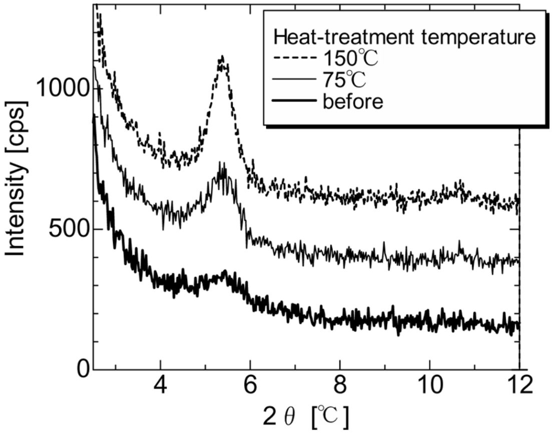

FIGURE 3 The X-ray diffraction patterns of active layer (P3HT/PCBM blend film) as a parameter of heat-treatment temperature.

as temperature increase above 100°C probably due to the decrease in shunt resistance. Figure 4 shows the comparison of the I-V curves of ITO/H-TiO_2/P3HT + PCBM/Au, ITO/H-TiO_2/P3HT + PCBM/MoO_3/Au

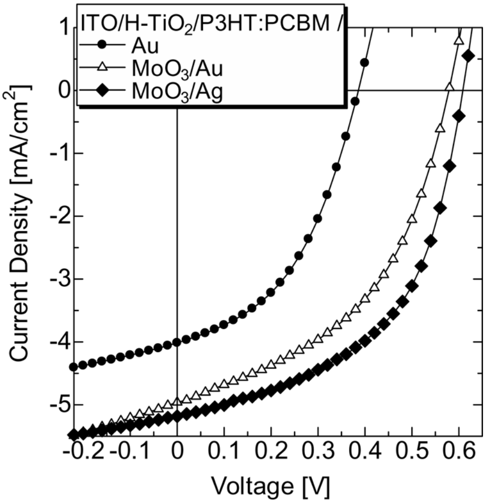

FIGURE 4 The comparison of the I-V curves of ITO/H-TiO_2/P3HT + PCBM/Au, ITO/H-TiO_2/P3HT + PCBM/MoO_3/Au and ITO/H-TiO_2/P3HT + PCBM/MoO_3/Ag devices under illumination. All samples were measured after heat-treatment at 75°C in a vacuum.

and ITO/H-TiO_2/P3HT + PCBM/MoO_3/Ag devices under illumination. Here, all samples were measured after heat-treatment at 75°C in a vacuum. Both open circuit voltage V_{OC} and short circuit current density J_{SC} markedly increase by the insertion of MoO_3 layer. We considered it is attributed to the increment of internal electric field between TiO_2 and top electrodes because MoO_3 has a larger work-function (>5 eV) than Au (4.8 eV) and Ag (4.4 eV) [22]. It should be noted here that Au particles penetrates into the organic film during the evaporation [23]. MoO_3 film, therefore, also contributes to reduce the penetration of Au and Ag into the active layer, and acts as the electron blocking layer. Figure 5 shows the change in V_{OC}, J_{SC}, fill factor (F.F.), and the power conversion efficiency η_P as a function of heat-treatment temperature for the devices discussed in Figure 4. The J_{SC} and η_P increase markedly by heat-treatment up to 75°C for all devices probably due to the crystallization of P3HT as discussed in Figure 3. On the other hand, V_{OC} decreases gradually with the heat-treatment temperature in the devices with MoO_3 buffer layer. It should be noted here that V_{OC} of ITO/H-TiO_2/P3HT + PCBM/MoO_3/Au and ITO/H-TiO_2/P3HT + PCBM/MoO_3/Ag are almost the same for all temperature though there is a remarkable difference in the work-function between Au (4.8 eV) and Ag (4.4 eV). We therefore considered that MoO_3 buffer layer acts as an electrode material and the work-function difference between TiO_2 and MoO_3 plays an

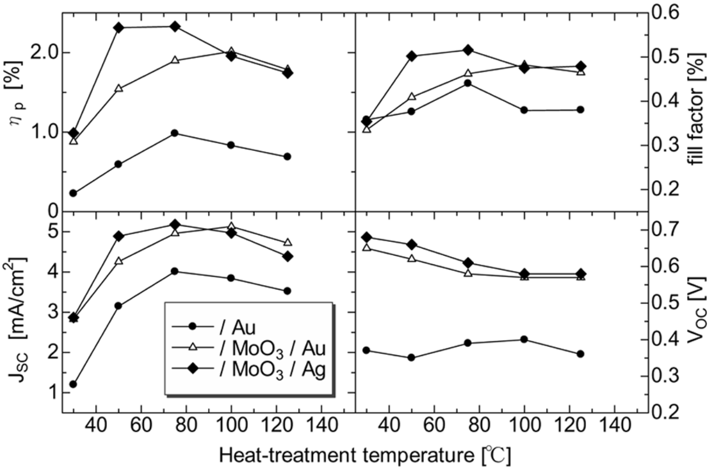

FIGURE 5 The change in open circuit voltage V_{OC}, short circuit current density J_{SC}, fill factor (F.F.), and the power conversion efficiency η_P as a function of heat-treatment temperature for the devices discussed in Figure 4.

important role for the V_{OC} of these devices. It should be noted here that the work-function of our MoO_3 film reduces its work-function from 5.2–5.4 eV to 4.7–4.8 eV by heat-treatment. Therefore, the decrease in V_{OC} at the heat-treatment temperature above 75°C is likely to due to the reduction of the built-in potential in the active layer. The mechanism should be clarified in the near future.

Figure 6 shows the I-V curves of ITO/L-TiO_2/P3HT + PCBM/MoO_3/Ag device as a parameter of the heat-treatment temperature under illumination. It is clearly shown that the photovoltaic properties were not so good compared with the device prepared on H-TiO_2 and J_{SC} decreases markedly by heat-treatment probably due to the electron trapping at L-TiO_2/active layer interface caused by the surface defect on TiO_2 film prepared by low-temperature process, such as –OH groups [24]. The results obtained in this device were not reproducible and the deviation between the samples were very large. Changes in the work-function of MoO_3 and the surface defect on TiO_2 layer may cause the reduction of V_{OC} during the heat-treatment. We therefore treated the surface of L-TiO_2 by fullerene based SAM, which is obtained by APTES and fullerene in toluene [21]. Figure 7 shows the comparison of the I-V curves of ITO/H-TiO_2/P3HT + PCBM/MoO_3/Ag, ITO/L-TiO_2/P3HT + PCBM/MoO_3/Ag and ITO/L-TiO_2/

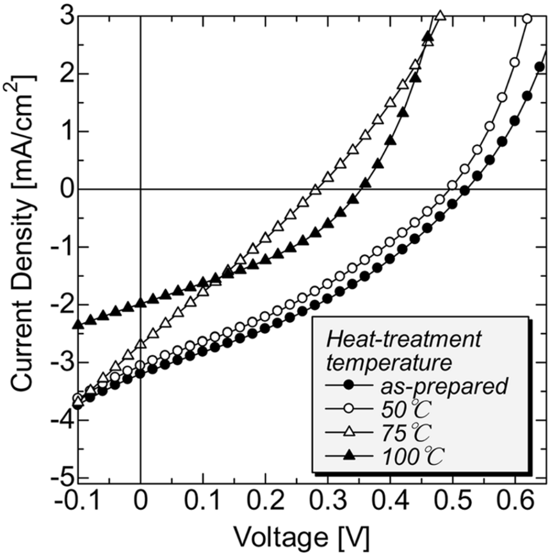

FIGURE 6 The I-V curves of ITO/L-TiO_2/P3HT + PCBM/MoO_3/Ag device as a parameter of the heat-treatment temperature under illumination.

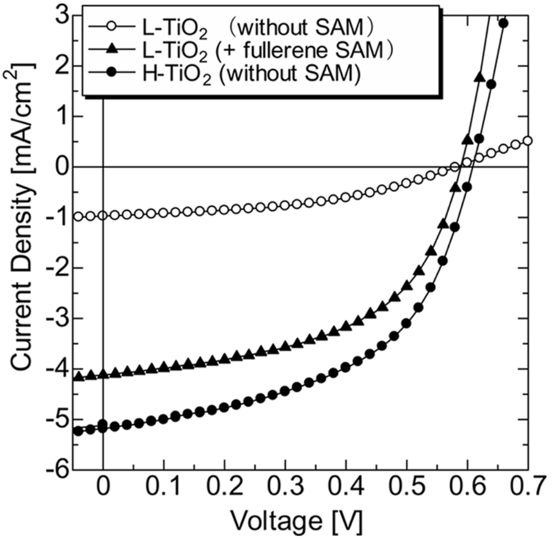

FIGURE 7 The comparison of the I-V curves of ITO/H-TiO_2/P3HT + PCBM/MoO_3/Ag, ITO/L-TiO_2/P3HT + PCBM/MoO_3/Ag and ITO/L-TiO_2/fullerene-based SAM/P3HT+PCBM/MoO_3/Ag devices under illumination.

fullerene-based SAM/P3HT + PCBM/MoO_3/Ag devices under illumination. Here, all samples in Figure 7 were measured after heat-treatment at 75°C in a vacuum. It should be noted here that the photovoltaic properties of ITO/L-TiO_2/fullerene-based SAM (C_{60}-SAM)/P3HT + PCBM/MoO_3/Ag device are improved markedly and the photovoltaic properties are much reproducible compared with the device without C_{60}-SAM. Table 1 summarizes the photovoltaic properties obtained in Figures 2, 4 and 7. The power conversion

TABLE 1 The Summary of Photovoltaic Properties in Figures 2, 4 and 7. (Light intensity 70 mW/cm^2, 75°C: Heat-Treatment Temperature, Measured at RT.)

Device structure	J_{SC} [mA/cm^2]	V_{OC} [V]	F.F.	η_P [%]
ITO/H-TiO_2/P3HT + PCBM/Au (as prepared)	1.20	0.37	0.36	0.23
ITO/H-TiO_2/P3HT + PCBM/Au (75°C)	4.01	0.39	0.44	0.99
ITO/H-TiO_2/P3HT + PCBM/MoO_3/Au (75°C)	5.13	0.57	0.48	2.01
ITO/H-TiO_2/P3HT + PCBM/MoO_3/Ag (75°C)	5.18	0.61	0.52	2.33
ITO/L-TiO_2/P3HT + PCBM/MoO_3/Ag (75°C)	0.97	0.59	0.44	0.36
ITO/L-TiO_2/C_{60}-SAM/P3HT + PCBM/MoO_3/Ag (75°C)	4.10	0.59	0.53	1.81

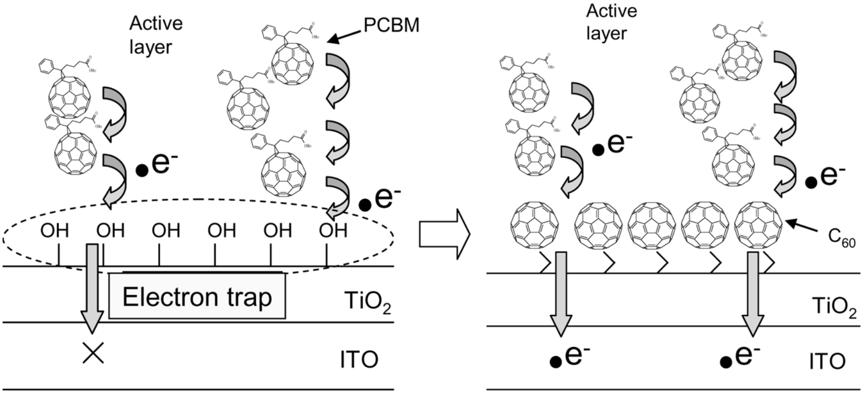

FIGURE 8 Schematic illustration of surface treatment of low-temperature processed TiO_2 film.

efficiency of ITO/L-TiO_2/C_{60}-SAM/P3HT + PCBM/MoO_3/Ag device (1.81%) was five times as large as that of the device prepared on L-TiO_2 without C_{60}-SAM (0.36%) and it was comparable to those of ITO/H-TiO_2/P3HT + PCBM/MoO_3/Ag device (2.33%), successfully. We therefore considered that the electron traps, such as –OH groups on the surface of TiO_2 is probably terminated by fullerene-based SAM and fullerene molecules assist the electron-transfer from PCBM to TiO_2 film (see Fig. 8).

4. CONCLUSIONS

We have prepared crystalline TiO_2 (anatase) thin films by the high-temperature process (500°C) and the low-temperature process at 150°C, which is suitable for the application of polymer electronics by sol-gel techniques. The refluxed sol of titanium tetraisopropoxide (TTI) with water and nitric acid formed anatase phase TiO_2 without requiring the high-temperature process. Both open circuit voltage and short circuit current density of ITO/H-TiO_2/P3HT:PCBM/Au (or Ag), which is fabricated on high temperature processed TiO_2 (H-TiO_2), were improved markedly by the insertion of MoO_3 buffer layer between the active layer and top electrode. The photovoltaic properties were also improved by the heat-treatment of up to 75°C before measurement in a vacuum which is attributed to the crystallization of P3HT. However, higher temperature leads to the decrease in device properties. The photovoltaic properties of the device fabricated on low-temperature processed TiO_2 (L-TiO_2) deteriorates markedly than the device on H-TiO_2 probably due to the surface defects, and it was improved markedly by the surface treatment of TiO_2 by fullerene based SAM. Therefore, it was concluded that the insertion of effective buffer layer and the surface treatment of oxide is very important for the device performance of inverted BHJ solar cells.

REFERENCES

[1] Sariciftci, N. S., Smilowitz, L., Heeger, A. J., & Wudl, F. (1992). *Science*, *258*, 1474.

[2] Yu, G., Gao, J., Hummelen, J. C., Wudl, F., & Heeger, A. J. (1995). *Science*, *270*, 1789.

[3] Brabec, C. J., Sariciftci, N. S., & Hummelen, J. C. (2001). *Adv. Funct. Mater.*, *11*, 15.

[4] Shaheen, S. E., Brabec, C. J., Sariciftci, N. S., Padinger, F., Fromherz, T., & Hummelen, J. C. (2001). *Appl. Phys. Lett.*, *78*, 841.

[5] Padinger, F., Rittberger, R., & Sariciftci, N. S. (2003). *Adv. Funct. Mater.*, *13*, 85.

[6] Ma, W., Yang, C., Gong, X., Lee, K., & Heeger, A. J. (2005). *Adv. Funct. Mater.*, *15*, 1617.

[7] Reyes-Reyes, M., Kim, K., & Carroll, D. L. (2005). *Appl. Phys. Lett.*, *87*, 083506.

[8] Kim, J. Y., Kim, S. H., Lee, H. H., Lee, K., Ma, W., Gong, X., & Heeger, A. J. (2006). *Adv. Mater.*, *18*, 572.

[9] Hayakawa, A., Yoshikawa, O., Fujieda, T., Uehara, K., & Yoshikawa, S. (2007). *Appl. Phys. Lett.*, *90*, 163517.

[10] Fujishima, A., Rao, T.N., & Tryk, D.A. (2000). *J. Photochem. Photobiol., C 1*, 1.

[11] Regan, B. O'. & Grätzel, M. (1991). *Nature*, *353*, 737.

[12] Bach, U., Lupo, D., Compte, P., Moser, J. E., Weissörtel, F., Salbeck, J., Spreitzer, H., & Grätzel, M. (1998). *Nature*, *395*, 583.

[13] Krüger, J., Plass, R., Grätzel, M., & Matthieu, H.. (2002). *Appl. Phys. Lett.*, *81*, 367.

[14] Arango, A. C., Johnson, L. R., Bliznyuk, V. N., Schlesinger, Z., Carter, S. A., & Hörhold, H. (2000). *Adv. Mater.*, *12*, 1689.

[15] Breeze, A. J., Schlesinger, Z., Carter, S. A., & Brock, P. J. (2001). *Phys. Rev. B*, *64*, 125205.

[16] Itoh, E., Ohmori, Y., & Miyairi, K. (2004). *Jpn. J. Appl. Phys.*, *43*, 817.

[17] Yun, Y. J., Chung, J. S., Kim, S., Hahn, S. H., & Kim, E. J. (2004). *Mater. Lett.*, *58*, 3703.

[18] Zhu, J., Bian, Z. F., Ren, J., Liu, Y. M., Cao, Y., Li, H. X., Dai, W. L., He, H. Y., & Fan, K. N. (2007). *Catal. Commun.*, *8*, 971.

[19] Itoh, E., Takamizawa, Y., & Miyairi, K. (2008). *Jpn. J. Appl. Phys.*, *47*, 509.

[20] Asanuma, T., Matsutani, T., Liu, C., Mihara, T., & Kiuchi, M. (2004). *J. Appl. Phys.*, *95*, 6011.

[21] Chen, K., Calddwell, W. B., & Mirkin, C. A. (1993). *J. Am. Chem. Soc.*, *115*, 1193.

[22] Shrotriya, V., Li, G., Yao, Y., Chu, C.-W., & Yang, Y. (2006). *Appl. Phys. Lett.*, *88*, 073508.

[23] Suemori, K., Miyata, T., Yokoyama, M., & Hiramoto, M. (2004). *Appl. Phys. Lett.*, *85*, 6269.

[24] Chua, L. L., Zaumseil, J., Chang, J. F., Ou, E. C. W., Ho, P. K. H., Sirringhaus, H., & Friend, R. H. (2005). *Nature*, *434*, 194.